Electron correlation effects and ferromagnetic order in β-UB_2C

2006 J. Phys.: Condens. Matter 18 703

(http://iopscience.iop.org/0953-8984/18/2/024)

INSTITUTE OF PHYSICS PUBLISHING JOURNAL OF PHYSICS: CONDENSED MATTER

J. Phys.: Condens. Matter **18** (2006) 703–718 doi:10.1088/0953-8984/18/2/024

Electron correlation effects and ferromagnetic order in β-UB_2C

V H Tran[1], P Rogl[2], G André[3] and F Bourée[3]

[1] W Trzebiatowski Institute of Low Temperature and Structure Research, Polish Academy of Sciences, PO Box 1410, PL-50-950 Wrocław, Poland
[2] Institut für Physikalische Chemie, Universität Wien, Währingerstrasse 42, A-1090 Wien, Austria
[3] Laboratoire Léon Brillouin, CEA/CNRS-Saclay, 91191 Gif-Sur-Yvette Cédex, France

Received 23 September 2005, in final form 7 November 2005
Published 16 December 2005
Online at stacks.iop.org/JPhysCM/18/703

Abstract

Measurements of the magnetic susceptibility, magnetization, electrical resistivity, magnetoresistance, specific heat, thermoelectric power and neutron powder diffraction on a polycrystalline sample of β-UB_2C are reported. It is found that this compound with enhanced electronic specific-heat coefficient is a ferromagnet below $T_C = 74.5(0.5)$ K. At 1.5 K the ordered magnetic moment of the uranium ions is found to be 1.12(1) μ_B (U1 in 3b) and 1.03(1) μ_B (U2 in 6c), respectively. The uranium moments are close to the ab-plane ($\Phi = 47°$ and $\Theta = 84°$) forming ferromagnetic chains parallel to the hexagonal c-axis. In addition to the ferromagnetic transition, we found a characteristic temperature $T^* = 37$ K, at which both the electrical resistivity and specific heat show anomalies. The thermoelectric power is positive and displays a maximum at 12 K. The observed features are compared to those of ferromagnetic UGe_2 and UIr, known as superconductors under pressure. We discuss the experimental data in terms of strong electron correlation effects.

(Some figures in this article are in colour only in the electronic version)

1. Introduction

Intermetallic 4f- or 5f-electron compounds exhibit a variety of exotic phenomena such as heavy-fermion, non-Fermi liquid, anisotropic superconductivity, and so on [1]. This is because the f-electron states in these materials are unstable and when RKKY interaction and Kondo effect compete with each other, heavy-mass quasi-particles may form at low temperatures. Since a few years ago when superconductivity in the ferromagnetic ground state of UGe_2 [2–4], and of URhGe [5], was discovered, a new view on 5f-electron magnetism has appeared in condensed matter physics. Although the 5f-electrons are believed to exhibit dual nature itinerant and localized ones [6–8], and therefore are considered to be responsible for both

magnetism and superconductivity, the most important aspect of these recent discoveries is that the Curie temperature T_C is always higher than the superconducting critical temperature T_{SC}. In the case of UGe_2, T_C is even two orders of magnitude higher than T_{SC}. Recently, superconductivity induced by pressure has been observed by Akazawa *et al* [9] in the itinerant electron ferromagnet UIr possessing a relatively high Curie temperature of $T_C = 46$ K. In view of the interesting behaviour of uranium compounds and also in order to study the role of strong electron correlations in metallic systems, it was considered fruitful to investigate fundamental properties of new ferromagnetic U-based intermetallics.

During the investigation of U–B–C system, the borocarbide UB_2C was found to exist in two modifications [10]. The low-temperature form, called α-UB_2C, crystallizes in the orthorhombic space group *Pmma* [11] whereas the high-temperature form, called β-UB_2C, adopts the rhombohedral ThB_2C-type structure (space group $R\bar{3}m$) [12]. Preliminary investigations on UB_2C indicated that the α form is a temperature-independent paramagnet, whilst the β form is ferromagnetic [13].

In this paper, we present details on the fundamental properties of β-UB_2C by means of measurements of magnetization, electrical resistivity, magnetoresistance, thermoelectric power and neutron powder diffraction. All the obtained data indicate strong correlation effects in the ferromagnetic compound β-UB_2C below $T_C = 74.5(0.5)$ K. Another interesting result is the occurrence of a characteristic temperature $T^* = 37$ K, resembling the behaviour of UGe_2 and UIr. For the latter compounds a superconducting state is formed when T^* is suppressed down to 0 K under pressure [3, 4, 9].

2. Experimental details

Following the procedure given in [13], a sample with a total weight of about 15 g was prepared by argon arc-melting the elements together on a water-cooled copper hearth using a non-consumable thoriated tungsten electrode in a protective Ti/Zr-gettered high-purity argon atmosphere. Uranium platelets of nuclear grade (E. Merck, Darmstadt, Germany) were surface cleaned prior to use in dilute nitric acid. Reactor-grade carbon (impurities <1.4 ppm, Carbone Lorraine, France) and crystallized boron (98.% ^{11}B-enriched isotope from Tbilisi, Georgia; impurities <6000 ppm) were used as powders which prior to arc melting were compacted in a steel die into tablet form. Weight losses were found to be less than 0.5% mass. Starting from a nominal composition, 23 at.% U, 51 at.% ^{11}B and 26 at.% C, an almost single phase and well-crystallized product was obtained containing minor amounts of $U^{11}B_4$ ($a = 0.7069(3)$, $c = 0.3967(3)$ nm) and graphite ($a = 0.2506(2)$, $c = 0.6716(5)$ nm). Precise lattice parameters and standard deviations were obtained from a least-squares refinement of room-temperature Guinier–Huber x-ray powder data, using monochromatic Cu Kα1 radiation with an internal standard of 6N-pure Ge ($a_{Ge} = 0.565\,7906$ nm at RT). Neutron powder diffraction in the temperature range 1.5–295 K was performed at the Orphée 14MW-reactor at the Laboratoire Léon Brillouin, Saclay using the G4-1 double-axis multicounter neutron powder diffractometer with a helium cryostat ($\lambda_n = 0.2426$ nm; resolution $\Delta d/d = 4 \times 10^{-3}$). Preferred orientation effects were minimized by powdering the sample in a WC/Co mortar to a grain size smaller than 30 μm. Precise atom parameters, occupation numbers and profile parameters were derived from a least-squares full-matrix Rietveld refinement routine [14]. Neutron scattering lengths were taken from a compilation by Sears in [15].

Magnetization, $M(T, H)$, was measured using a SQUID (Quantum Design MPMS) in fields up to $\mu_0 H = 5.5$ T and in the temperature range 1.7–350 K. Specific heat, $C_p(T)$, measurements were performed in the temperature range 1.8–100 K, using an adiabatic method. Electrical resistivity, $\rho(T)$, was measured in the temperature range 1.8–300 K, using a four-

probe dc-technique with a current of 10 mA. Magnetoresistance, MR, data were collected in the temperature range 2–100 K and in a fixed magnetic field of 10 T on zero-field-cooled samples. The isothermal MR data at 1.8 K were collected in fields up to 13 T. The direction of the applied magnetic fields was perpendicular to the current. Thermoelectric power, S, was measured with a steady-state method between 2 and 300 K.

3. Results and discussion

3.1. Structural properties

Employing the atom parameter set obtained from the single-crystal x-ray intensity data refinement of homologous ThB_2C [12], the refinement of the neutron data straightforwardly converged, confirming crystal symmetry, atom site occupation and thus isotypism with the crystal structure of ThB_2C. In β-UB_2C, the U atoms occupy two distinct positions: U1 at 3b (0, 0, 1/2) and U2 at 6c (0, 0, z_U), while the boron atoms are located at the 18f (x_B, 0, 0) and carbon atoms at the 9e (1/2, 0, 0) sites (standardized hexagonal setting calculated via program *Structure Tidy* [16]). The crystal refinement with 60 independent reflections converged to a reasonable level with a fine agreement between the observed and calculated intensities ($R_B = 0.049$; $R_F = 0.028$) and diffraction profiles ($R_p = 0.084$). The refined structural parameters from the neutron powder diagram at RT are as follows: $a = 0.6530(2)$, $c = 1.0764(7)$ nm, $z_U = 0.1886(12)$ and $x_B = 0.2680(8)$. The occupancies of all atom sites have been refined; however, no significant deviation from a full occupation was revealed.

It follows from the crystal structure shown in figure 1 that the U atoms form slightly puckered hexagonal layers sandwiched between planar non-metal layers consisting of B_6- and B_6C_3-rings with linear B–C–B segments. The neutron diffraction data confirm the covalent B–B bonds ($d_{B-2B} = 0.1750$ nm) as well as the double bond between boron and carbon atoms, $d_{B-C} = 0.1515$ nm. Interestingly, the metal coordination around the two uranium atoms U1 and U2 is slightly different. Each U1 has one nearest neighbour U2 along the c-axis at the U–U distance, $d1_{U-U} = 0.3352$ nm, as many as six next-nearest neighbours (3U1 + 3U2) within the puckered layers at $d2_{U-U} = 0.3777$ and $d3_{U-U} = 0.3800$ nm, respectively and a far neighbour U1 at $d4_{U-U} = 0.4060$ nm. The U2 atoms have two close U1 neighbours at $d1_{U-U} = 0.3352$ nm in the direction of the c-axis, and six further U1 at $d2_{U-U} = 0.3777$ nm within the puckered metal layer.

3.2. Magnetic susceptibility and magnetization

Figure 2 shows the temperature dependence of the reciprocal magnetic susceptibility $\chi^{-1}(T)$ for β-UB_2C measured in a field of 0.5 T. The data were collected on two samples: on the virgin bulk and powdered ones. The results of the first are believed to represent the magnetic response of polycrystal, whereas the results of the latter could correspond to that measured along the easy magnetization direction. The $\chi^{-1}(T)$ curves of both samples deviate from the linear dependence at high temperatures, implying that the experimental data may follow a modified Curie–Weiss law (MCW):

$$\chi(T) = \frac{C}{T - \Theta_p} + \chi_0 \tag{1}$$

where C is a constant related to the effective moment μ_{eff} by a relation: $C = \frac{N_A g^2 \mu_{eff}^2 \mu_B^2}{3k_B}$, Θ_p is the paramagnetic Curie temperature, and χ_0 is a temperature-independent term. The fit of experimental data in the temperature range 115–350 K yields the following parameters:

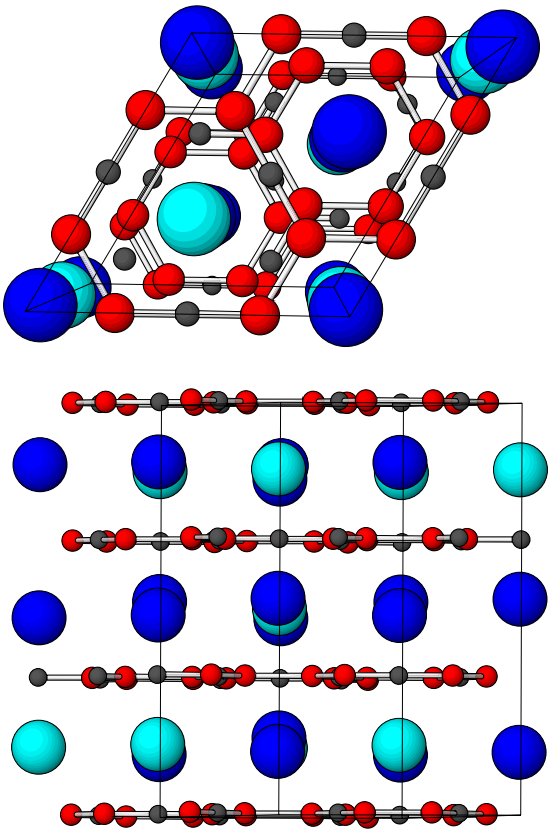

Figure 1. Crystal structure of β-UB_2C in three-dimensional view along the c-axis and the a-axis, respectively (top panel), revealing the planar $B_6 + B_6C_3$ non-metal network between the puckered hexagonal U-metal layers (bottom panel). Large, middle-size and small circles represent the uranium, boron and carbon atoms, respectively.

$\mu_{\mathrm{eff}} = 1.45(1)\ \mu_{\mathrm{B}}$/U, $\Theta_{\mathrm{p}} = 75(1)$ K and $\chi_0 = 0.6 \times 10^{-3}$ cm^3 mol^{-1} for the bulk sample and $\mu_{\mathrm{eff}} = 2.12(1)\ \mu_{\mathrm{B}}$/U, $\Theta_{\mathrm{p}} = 66(1)$ and 1.2×10^{-3} cm^3 mol^{-1} for the powdered sample. The previously reported μ_{eff}-value (1.89 μ_{B}) [13] lies between those of the bulk and powdered samples. The observed μ_{eff}-values for β-UB_2C are essentially small if compared to those of free U^{3+} or U^{4+} ions (3.62 μ_{B} or 3.58 μ_{B}). This fact may point to a strong hybridization of the 5f-electrons with the conduction band. The large and positive Θ_{p}-value may indicate a strong ferromagnetic interaction in the compound. The parameter χ_0 usually describes a contribution of the conduction electrons, but in the case of polycrystalline sample data, one should be careful to attach quantitative information to it. The effect associated with the averaging over possible orientations of crystallites in the sample leads χ_0 to have higher values than those originating from the contribution of the conduction electrons alone. Similarly, the μ_{eff}-values obtained by fitting to the MCW law are often smaller than the intrinsic effective moments.

Below 75 K, the magnetization rapidly increases due to the onset of ferromagnetic order, which is clearly evidenced by the minimum of the temperature derivative of the magnetization shown in the inset of figure 2. We may estimate the Curie temperature, T_{C}, to be 74.8 K, as the inflexion point of the $M(T)$-curve measured at a low field of 0.05 T. For a typical ferromagnet, applied magnetic fields shift the inflexion point to higher temperature.

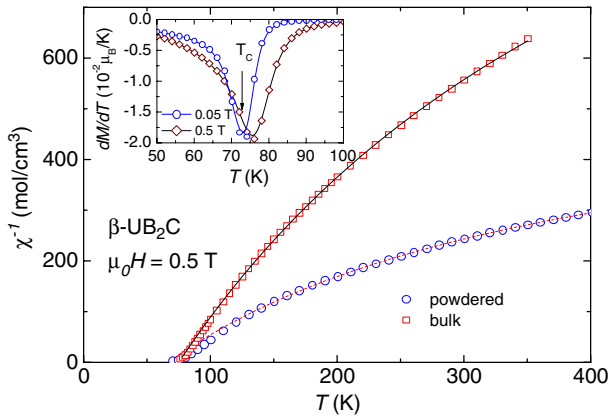

Figure 2. Temperature dependence of the inverse magnetic susceptibility of the bulk and powdered samples of β-UB_2C. The solid and dashed lines are the fit using a modified Curie–Weiss law. Inset: temperature dependence of the derivative dM/dT for magnetization measured at 0.05 and 0.5 T.

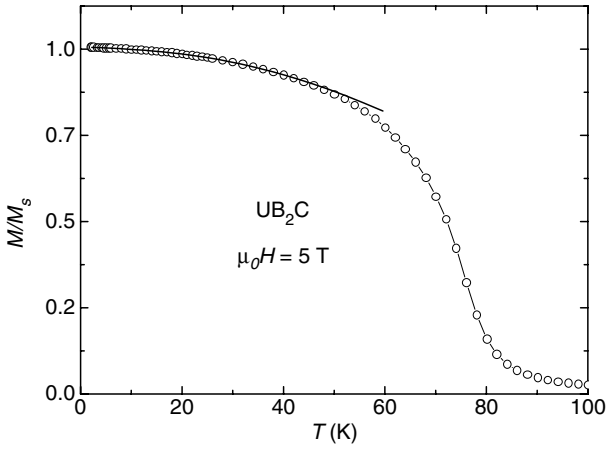

Figure 3. Temperature dependence of the magnetization measured at 5 T. The solid line is the fit based on the spin-wave theory.

The magnetization data (figure 3) below 40 K may be analysed with the help of the equation predicted by the spin-wave theory [17–19].

$$\frac{M(T)}{M_s} = 1 - BT^{3/2} - CT^{5/2} \tag{2}$$

where the coefficient B is related to the spin-wave stiffness constant D, through $B = 2.612(g\mu_B/M(0))(k_B/4\pi D)^{3/2}$ (g is the Landé factor, μ_B is the Bohr magneton and k_B is the Boltzmann constant). However, the studied compound crystallizes in a rhombohedral structure, so one might expect a strong magnetocrystalline anisotropy, which could manifest itself as an anisotropy gap Δ. This contribution to the total magnetization can be estimated from the equation [19, 20]:

$$\frac{M(T)}{M_s} = 1 - BT^{3/2}\exp(-\Delta/k_BT). \tag{3}$$

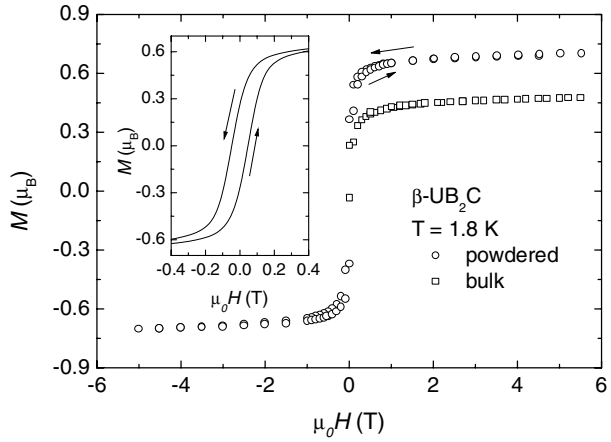

Figure 4. The magnetization of the bulk and powdered samples measured at 1.8 K. The inset shows the magnetization at low fields. The rightwards and leftwards arrows indicate the directions of increasing and decreasing magnetic field strength, respectively.

The fit of equation (3) for the data in the temperature range 2–35 K gives $B = 4 \times 10^{-4}$ K$^{-3/2}$ and $\Delta/k_B = 11(1)$ K. The result of the fit is shown as the solid line in figure 3. It should be noted that the derived value of Δ is rather small in view of large magnetocrystalline anisotropy of the order of 100 K, that is typically found in U-based systems [21]. This suggests that the magnetic excitations in β-UB_2C can have a complex nature and the deduced gap value must be confirmed by other experimental methods.

Taking $g = 0.67$ for U^{3+}, $V = 397$ Å^3, a saturation moment of 0.78 μ_B (see below) and the value of B, we have estimated the value of the spin-wave stiffness coefficient D to be 26 meV Å^2. Furthermore, the ratio $\frac{D}{k_B T_C}$ characterizing the nearest-neighbour exchange interaction strength amounts to about 4 Å^2. This value is comparable to those observed in other ferromagnets such as Fe, YFe_2, $CeFe_2$ and UFe_2 [22]. A relative large $\frac{D}{k_B T_C}$-value is characteristic of itinerant ferromagnets [23].

In figure 4 we show the magnetization measured at 1.8 K for the bulk and powdered samples. Apparently, the hysteresis is too small to be identified. In fact, in an enlarged scale (see inset of figure 4) one sees a low remanence (0.25 μ_B) and small coercivity (less than 200 Oe) in the powdered sample. The difference in the magnetic behaviour between these samples appears in the magnetization at high fields. For instance the M at 1.8 K and 5.5 T M reaches a value of 0.48 μ_B for the bulk sample but it attains 0.70 μ_B for the powdered one. This difference seems to have the same origin as in the case of the μ_{eff}-values and probably it is caused by the magnetocrystalline anisotropy and texture effect. The previously reported value (0.64 μ_B [13]) is close to that of the powdered sample. We have estimated the saturation moment of β-UB_2C to be 0.78 μ_B by plotting the magnetization of the powdered sample at 1.8 K against $1/H$ and extrapolating $1/H$ to zero. However, compared to the value expected for the U^{3+} ions (3.6 μ_B) the saturation magnetization of β-UB_2C is considerably smaller. This feature may result either from an itinerant nature of the uranium moments or an imbalance between the two magnetic sublattices, associated with a ferrimagnetic ground state. However, the latter has not been confirmed by either an Arrott plot analysis or by neutron powder diffraction experiments (see below). Taking into account all facts of a low remanence, small coercivity and small saturation magnetization, β-UB_2C may be a soft magnet.

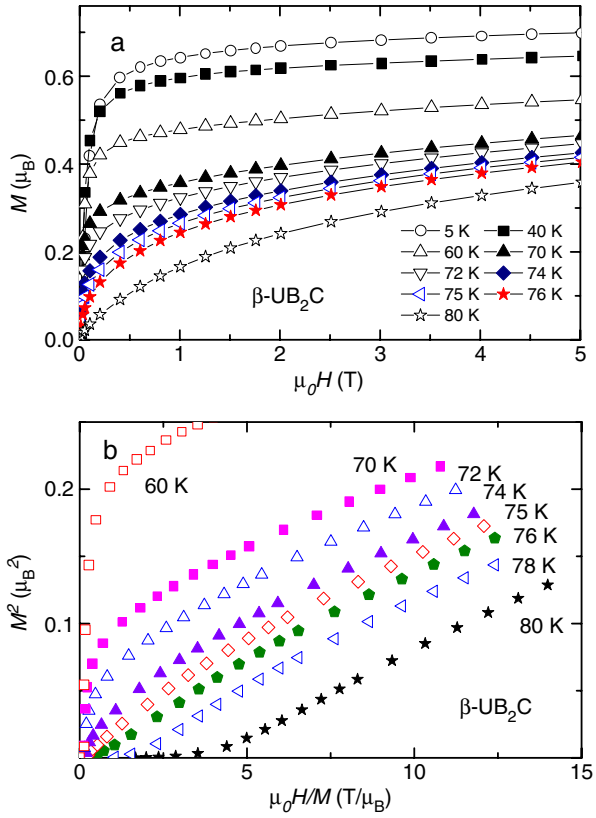

Figure 5. (a) The magnetization of the powdered sample measured at several selected temperatures below 80 K. (b) The M^2 versus H/M plots for the isotherms close to T_C.

In figure 5 (a) we show the magnetization isotherms measured below 80 K for the powdered sample. All isotherms below 60 K display a similar dependence characterized by a saturation at high fields. The magnetization data taken between 70 and 76 K vary in a manner typical for a weak ferromagnet and the magnetization curve at 80 K corresponds to that of material with a strong ferromagnetic correlation.

In order to gain insight into the nature of the magnetic ground state of the studied compound, the isotherm data were analysed with the help of the Arrott plot. In the simple mean-field case, the M^2 versus H/M dependence at various temperatures should show a series of parallel lines in accordance with the magnetic equation of state of the form $M^2 = A + B * H/M$. For ferromagnets, the coefficient $A > 0$ in the ordered state, but $A < 0$ in the paramagnetic state and $A = 0$ at the Curie temperature. As can be seen in figure 5(b), the isotherms below 75 K show positive A, i.e., there exists a spontaneous magnetization, which evidences that a ferromagnetic state sets in in the compound. For β-UB_2C, however, some deviation from linearity is clearly seen in these isotherms. Nevertheless, according to Arrot and Noakes [24], one improves the linearity of the isotherms by varying the critical exponents β and γ in the equation:

$$H/M^{1/\gamma} = \frac{T - T_C}{T_1} + \left(\frac{M}{M_1}\right)^{1/\beta}. \tag{4}$$

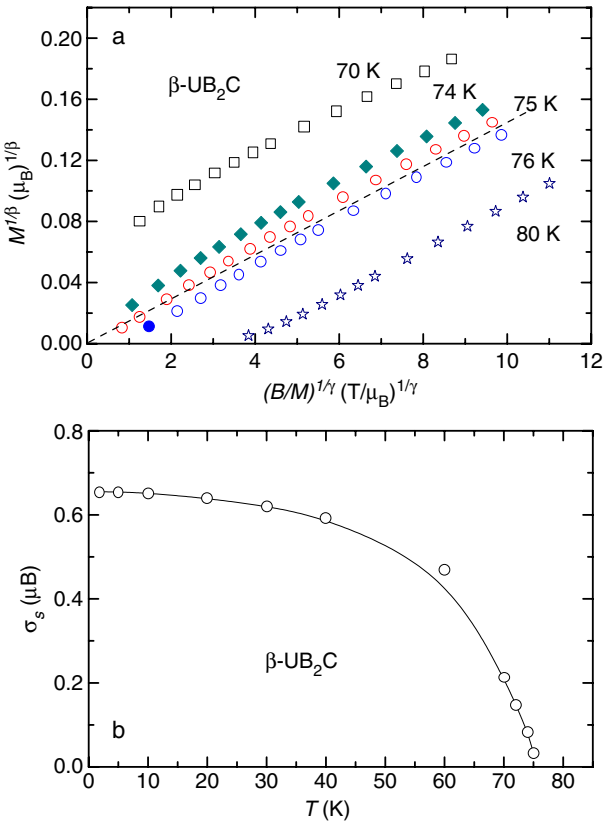

Figure 6. (a) Modified Arrott plots of isotherms for temperatures near T_C. The dashed lines illustrate the validity of the modified Arrott plot. (b) Temperature dependence of spontaneous magnetization derived by the modified Arrott plots.

Such an expression does contain the information on spontaneous magnetization σ_s below T_C

$$\sigma_s \sim (T_C - T)^{\beta} \tag{5}$$

and the inverse susceptibility just above T_C where T_1 and M_1 are constants. The fitting of the experimental data to equation (4) yields $\beta = 0.455(2)$ and $\gamma = 1.10(1)$. Based on these parameters the modified Arrott plots (figure 6(a)) can be constructed. The isotherms now are almost straight lines, and then they could prove the validity of the choice of β and γ. From figure 6 we have derived the spontaneous magnetization which is shown in figure 6(b) as a function of temperature. This figure allows us to evaluate the value of the Curie temperature to be of 75.2(3) K.

3.3. Magnetic structure

The powder patterns observed below T_C reveal no new diffraction peaks; however, significant intensity changes are observed when compared to the 100 K pattern. The most prominent contributions of magnetic origin are observed for (003), (110), (113), (311) and (300) reflections. With decreasing temperature, the intensities of the magnetic peaks increase in the manner shown in the inset of figure 7. The temperature dependence of the intensity of the magnetic peak (110) yields T_C, which is in good agreement with that determined in the

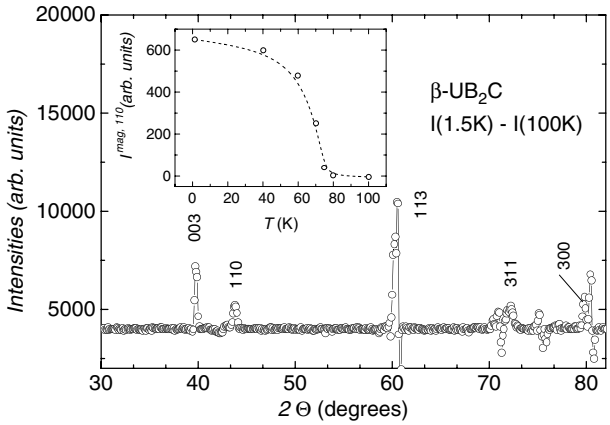

Figure 7. Difference between neutron power diffraction patterns taken at 1.5 and 100 K. The solid line is a guide for the eye. The inset shows the temperature dependence of the intensity of the magnetic peak (110).

Table 1. Observed and calculated intensities of the magnetic reflections in β-UB_2C at 1.5 K.

hkl	I_{obs}	I_{cal}
003	1085	912
110	649	649
113	3287	3286

magnetic susceptibility, electrical resistivity and heat capacity studies. In figure 7 we show the difference between pattern collected at 1.5 and 100 K. However, the resolution of two higher-angle reflections is limited. Thus, to elucidate the magnetic structure, we have taken into account the intensities of the first three magnetic reflections only. Employing Monte Carlo methods [14], the magnetic structure of β-UB_2C at 1.5 K was resolved as being a colinear ferromagnet with ordered magnetic moments for both the uranium sites close to the ab-plane. With free variables for the size and the coupled direction of the uranium moments, the refinements (table 1) converged at the magnetic R-factor of 0.140 and $M(\mathrm{U1}) = 1.12(1)\ \mu_B$, $M(\mathrm{U2}) = 1.03(1)\ \mu_B$, and $\Phi = 47(1)^\circ$ and $\Theta = 84(2)^\circ$. Φ and Θ are the spherical angles referred to the crystal axes x and z, respectively. The small deviation of Θ from 90° accounts for the puckering of the uranium metal layers. Inspecting the fitted moments, we see a slight difference between $M(\mathrm{U1})$ and $M(\mathrm{U2})$, which is believed to be of no significance. An average value of 1.06 μ_B/U-atom is in agreement with that obtained from the magnetization on the powdered sample (0.78 μ_B) if one takes into account that the saturation moment observed in a powder is $\pi/4$ of the easy-plane value in an easy-plane system. In figure 8 we illustrate the arrangement of the uranium ions. However, we must admit that with the few magnetic peaks available the magnetic structure may be more complicated than the simple model suggests. In particular, due to the presence of the two crystallographically inequivalent U sites, the occurrence of a ferrimagnetic order cannot be excluded at present. The proper magnetic structure can only be ascertained from large single crystals, which are not available.

3.4. Specific heat

In figure 9 we show the specific heat divided by temperature C_p/T of β-UB_2C below 100 K. The sharp peak near 75 K is consistent with the ferromagnetic transition implied by magnetic

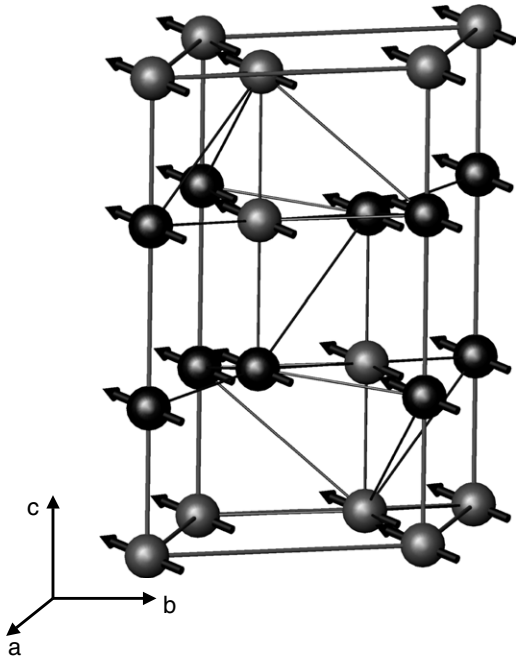

Figure 8. Magnetic structure of βUB_2C. Only the uranium ions are shown.

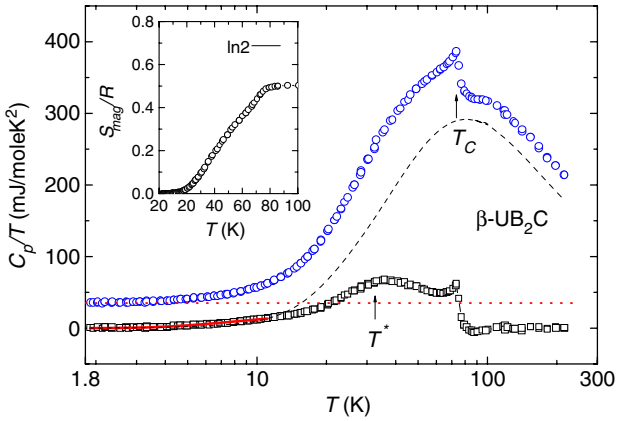

Figure 9. Temperature dependence of the specific heat divided by temperature. The dotted and dashed lines present the electronic and phonon contributions, respectively. The open squares present the magnetic contribution, $C_{\rm mag} = C_{\rm p} - C_{\rm el} - C_{\rm ph}$. The solid line is the fit (see text).

and resistivity (see below) measurements. The specific heat data in the temperature range 2–8 K may be analysed as a sum of two different contributions: the electronic $C_{\rm el}$ and phonon $C_{\rm ph}$ contributions, which are assumed to be dependent on temperature as $C_{\rm el}(T) = \gamma T$ and $C_{\rm ph}(T) = \beta T^3$, respectively. From the fit of the experimental data we obtained $\gamma = 34.7(2)$ mJ mol^{-1} K^{-2} and $\beta = 0.25(1)$ mJ mol^{-1} K^{-4}. The first value allows us to estimate the electronic density of states at the Fermi level $N(E_{\rm F})$ assuming

$$\gamma = \tfrac{1}{3}\pi^2 k_{\rm B}^2 N(E_{\rm F}). \tag{6}$$

Using the above equation we obtained $N(E_F) = 14.7\ \mathrm{eV}^{-1}/\mathrm{atom}$. From the coefficient of the electronic specific heat and the jump of C_p at T_C we obtained $\frac{\Delta C_p}{\gamma T_C} = 2$. The latter value is remarkably larger than the BCS value of 1.43. Because the BCS theory developed for superconductors with a weak coupling, any deviation from the BCS value may indicate a strong correlation between electrons.

In a strong coupling regime, the BCS ratio has been corrected by Allen and Dynes, who took into account the coupling parameter λ, which is proportional to the density of state [25]. Note that both the phonon–electron λ_{e-ph} and electron–electron λ_{e-e} coupling parameters are associated with the effective electron mass.

Through the relation

$$\beta = \frac{12}{5} R\pi^4 \left(\frac{T}{\Theta_D}\right)^3. \tag{7}$$

we determined the Debye temperature to amount to $\Theta_D = 314$ K.

In order to ascertain the nature of magnetic state one needs to separate the magnetic contribution from the others, i.e., by subtracting the phonon and electronic contributions from the total specific heat. However, for β-UB_2C, there is still a lack of a suitable non-f-electron reference compound. Therefore, in the first approximation we assumed C_{ph} to be described by the Debye function: $C_{ph} = \frac{9N_A k_B T^3}{\Theta_D^3} \int_0^{\Theta_D/T} \frac{x^4 \exp(x)}{(\exp(x)-1)^2} dx$ with Θ_D deduced from the low-temperature data. Bearing in mind that the Debye function works only for $T < \Theta_D/50$ and $T > \Theta_D/2$, we further have taken into account the Einstein contribution, which is seen when plotting the ratio C_p/T^3 versus T. The presence of a broad maximum at 22 K with an amplitude of 0.52×10^{-4} J mol^{-1} K^{-4} in the C_p/T^3 versus T curve implies the existence of the Einstein contribution with an Einstein temperature of $\Theta_E = 110$ K and a number of Einstein vibrators of $n_E = 0.18$. Including the electronic and phonon contributions we simulated their contributions as the dashed line in figure 9. The magnetic contribution shown in figure 9 as open points was deduced from the relation $C_{mag} = C_p - C_{ph,D} - C_{ph,E} - C_{el}$. From this figure one recognizes that there is a considerable contribution of C_{mag} to the total specific heat, especially for temperatures around $T^* = 35$ K, where C_{mag} displays a prominent maximum. This anomaly should be confirmed by any future studies when the proper phonon contribution will be available. Nevertheless, the observed feature resembles the behaviour of the ferromagnetic superconductor UGe_2 [4, 26], for which a hump around 30 K in C_{mag}/T has been attributed to the Kohn effect [27], associated with the coupled charge-density wave and spin-density wave ordering. Alternatively, a maximum in the specific heat below T_C might be observed due to the quantum fluctuations of the spin. This behaviour has been predicted by Fishman and Liu in the Heisenberg model of ferromagnetism [28]. Besides these mechanisms mentioned above we would like to add that the specific heat of magnetically ordered systems may show a hump below their $T_{C/N}$ if the angular momentum J is larger than $1/2$. This fact can be explained in mean-field theory by Zeeman splitting of a high-J state owing to the strong molecular field. Examples of such a behaviour are compounds based on Gd [29, 30].

The magnetic specific heat data of β-UB_2C might be analysed within the model developed by Andersen and Smith for the electron–magnon scattering in ferromagnets [31]. According to this model, the magnetic contribution to the total specific heat is given by $C_{mag}(T) = \sigma T^{0.5} \exp(-\Delta/k_B T)$, where Δ is the energy gap in the magnon spectrum. For the experimental data between 2–10 K, the fit is shown in figure 9 as a solid line. We obtained fitting parameters $\sigma = 0.17$ J mol^{-1} K$^{-1.5}$ and $\Delta = 14.8(5)$ K. The latter value is consistent with the gap determined from the magnetization data. Comparing to the gap values found in other uranium ferromagnets, for instance in UPt (35 K) [32, 33], UPtAl (55 K) [34] and $UAuSb_2$ (61 K) [35], we suspect that a large excitation energy occurs in compounds with a huge magnetocrystalline

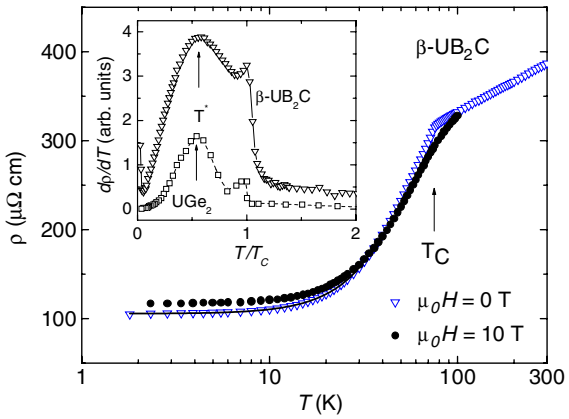

Figure 10. Temperature dependence of the electrical resistivity at 0 and 10 T. The solid lines present the fit of data (see text). The inset shows the temperature derivative of the resistivity $\mathrm{d}\rho(T)/\mathrm{d}T$ as a function of the reduced temperature T/T_{C}. These data are compared to those measured on a single-crystal UGe_2 from [36].

anisotropy. The small value of gap for β-UB_2C is probably due to a strong hybridization of the 5f states with other states in the compound.

The magnetic specific heat data presented above allow us to estimate the magnetic entropy S_{mag} (see the inset of figure 9). At T_{C}, S_{mag} approaches 72% of the value of $R \ln 2$, as expected for a doublet ground state. In the case of absence of the Kondo effect, the reduction in the magnetic entropy is interpreted in terms of strong hybridization of the localized 5f-electron state with the itinerant conduction electron state.

3.5. Transport properties

The electrical resistivity of β-UB_2C measured at 0 and 10 T as a function of temperature is depicted in figure 10. Some interesting features are observed in the $\rho(T)$-curves: (i) a sharp drop in the $\rho(T)$-curve at 0 T below 74.5 K supporting the onset of ferromagnetic order, (ii) the magnetoresistance is positive at temperatures below ∼40 K, and (iii) this temperature coincides with a broad hump visible as a pronounced maximum in the temperature derivative of the resistivity $\mathrm{d}\rho(T)/\mathrm{d}T$. The occurrence of the maximum of $\mathrm{d}\rho(T)/\mathrm{d}T$ of β-UB_2C at $T^* = 37$ K quantitatively resembles that of UGe_2 [36], and UIr [37]. This similarity is illustrated by plotting the derivative $\mathrm{d}\rho(T)/\mathrm{d}T$ versus the reduced temperature T/T_{C} (see the inset of figure 10). Clearly, for both β-UB_2C and UGe_2 intermetallics, the ratio T^*/T_{C} approaches 0.55. We recall that for UGe_2 under a pressure of 1.2 GPa, T^* becomes suppressed to zero [36], and simultaneously superconductivity was found [2].

The resistivity data of β-UB_2C at 0 T and in the temperature range 2–30 K may be fitted with the equation

$$\rho(T) = \rho_0 + AT^2 + bT\left(1 + \frac{2k_{\mathrm{B}}T}{\Delta}\right)\exp\left(-\frac{\Delta}{k_{\mathrm{B}}T}\right). \tag{8}$$

In this equation ρ_0 is a temperature-independent term representing the defect scattering, the second term is a Fermi-liquid-like contribution, and the last term is given in [31] for the electron–magnon scattering process. In the fitting we fixed the magnon gap at the value of 15 K deduced from the specific heat measurement and residual resistivity $\rho_0 = 105.5\ \mu\Omega$ cm.

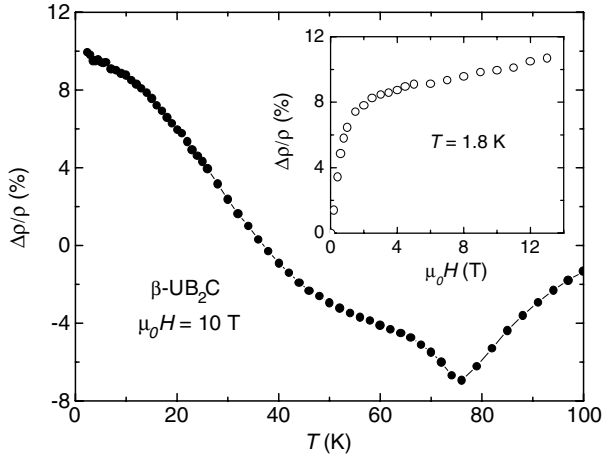

Figure 11. Temperature dependence of the magnetoresistance measured at 10 T. The inset shows the magnetoresistance at 1.8 K as a function of field up to 13 T.

The result of the fit with $A = 0.04(1)\ \mu\Omega$ cm K^{-2} and $b = 0.172(3)\ \mu\Omega$ cm K^{-1} is indicated as a solid line in figure 10. Using the relation given by Kadowaki and Woods (KW) [38], and the above values for A and γ, we find the ratio $r_{\mathrm{KW}} = A/\gamma^2 = 3.32 \times 10^{-5}\ \mu\Omega\,\mathrm{cm}/(\mathrm{mJ/mol\ K^2})^2$ for β-UB_2C. This is much higher than the common value of $1 \times 10^{-5}\ \mu\Omega\,\mathrm{cm}/(\mathrm{mJ/mol\ K^2})^2$ for heavy-fermion compounds. The origin of the enhanced r_{KW} ratio in β-UB_2C is not understood at present. However, for intermetallic compounds, there are several mechanisms leading to an enlargement of the KW ratio. As pointed out by Takimoto and Moriya [39], the large r_{KW} ratio may be ascribed to the effect associated with spin fluctuations. On the other hand, Miyake *et al* [40] have shown that the effect of many-body correlations in heavy-fermion systems can enhance the r_{KW}-value to even 25 times larger than that in the case of a single-body band. Finally, enhanced values of r_{KW} are also found to be due to an enhanced magnitude of the electron–electron scattering resulting from the magnetic frustration or from the proximity of a nearby magnetic quantum critical point, such as these recently observed, for instance, in $YbRh_2Si_2$ [41] and $CeCoIn_5$ [42].

From the data collected at 10 T, it is clear that the field suppresses critical fluctuations at T_{C}, smearing out the ferromagnetic transition. Comparing the temperature dependences of the derivative $\mathrm{d}\rho(T)/\mathrm{d}T$ at 0 and 10 T we observe that the position of T^* seems to be little increased by the field. At a field of 10 T, the resistivity at low temperatures still follows equation (8). A remarkable feature is also that the applied field increases the residual value up to 116 $\mu\Omega$ cm, resulting in a positive magnetoresistance of 10% (see figure 11). A positive magnetoresistance has also been reported for UGe_2 at low temperatures [43–46]. In the case of β-UB_2C we observe the sign change in the magnetoresistance near T^*.

The thermoelectric power S of β-UB_2C is displayed in figure 12. S is positive at all measured temperatures. No clear anomaly near T_{C} is found, indicating a negligible magnetic contribution to S. Interestingly, S displays a maximum at about 12 K. The origin of this phenomenon is not clear at present, but this tracks the thermoelectric power behaviour of UGe_2 at 10 K [47]. At temperatures below 10 K, the $S(T)$ dependence takes the form

$$S = \alpha T + \beta T^{3/2} \tag{9}$$

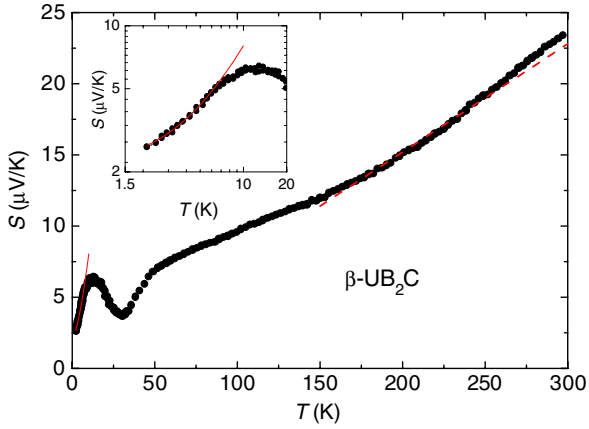

Figure 12. Temperature dependence of the thermoelectric power. The solid line is a fit, while the dashed line is the calculated diffusion thermopower. The inset shows $S(T)$ at low temperatures. The solid line is a fit.

in consistency with that predicted for ferromagnets by the spin-wave theory. At high temperatures, S depends approximately linearly on T. Such a dependence is expected for the diffusion thermopower in the case of dominant electron–phonon scattering. We have measured the Hall coefficient R_{H} at room temperature and have found R_{H} to amount to 1.44×10^{-9} m^3 C^{-1}. The positive thermopower and Hall coefficient suggest that hole-type carriers dominate the transport properties of β-UB_2C. In the free-electron approximation, the diffusion thermopower varies with temperature as $S_{\mathrm{d}} = [2k_{\mathrm{B}}^2 m_e]/[e\hbar^2(3n\pi)^{2/3}]T$. Using the charge-carrier concentration $n = 1/eR_{\mathrm{H}}$ extracted from the Hall coefficient at 300 K and assuming the electron mass m_e to be that of the free electron, we calculated S_{d}. The dashed line shown in figure 12 fits well to the experimental data.

4. Summary

In summary, by means of the magnetization, specific heat, resistivity and neutron powder diffraction measurements we have confirmed that β-UB_2C orders ferromagnetically below 74.5($\pm$0.5) K. We have demonstrated that the electronic specific heat coefficient of this compound is enhanced. Together with the reduced magnetic entropy at T_{C} and the small value of the ordered uranium moment, all these features strongly indicate that the 5f-electrons in β-UB_2C hybridize with the conduction electrons. In the ferromagnetic state, the transport and thermodynamic properties are found to be governed by a combination of the electron scattering on magnons and an additional mechanism revealing a characteristic temperature T^*. The latter feature resembles that of UGe_2 and UIr, and further investigations, notably measurements of the electrical resistivity under pressure, are planned to clarify it.

Acknowledgments

The authors acknowledge the support from an Austrian–Polish Scientific Exchange Program 19/2003. One of us (VHT) also thanks the Polish State Committee for Scientific Research for support within grant No. 4T08A 045 24.

References

[1] Steglich F and Süllow S 2001 *Encyclopedia of Materials: Science and Technology* (Amsterdam: Elsevier) p 3746
Löhneysen H v 2001 *Encyclopedia of Materials: Science and Technology* (Amsterdam: Elsevier) p 6185
[2] Saxena S S, Agarwal P, Ahilan K, Grosche F M, Haselwimmer R K W, Steiner M J, Pugh E, Walker I R, Julian S R, Monthoux P, Lonzarich G G, Huxley A, Sheikin I, Braithwaite D and Flouquet J 2000 *Nature* **406** 587
[3] Tateiwa N, Kobayashi T C, Hanazono K, Amaya K, Haga Y, Settai R and Onuki Y 2001 *J. Phys.: Condens. Matter* **13** L17
[4] Huxley A, Sheikin I, Ressouche E, Kernavanoi N, Braithwaite D, Calemczuk R and Flouquet J 2001 *Phys. Rev.* B **63** 144519
[5] Aoki D, Huxley A, Ressouche E, Braithwaite D, Flouquet J, Brison J-P, Lhotel E and Paulsen C 2001 *Nature* **413** 613
[6] Sato N K, Aso N, Miyake K, Shiina R, Thalmeier P, Varelogiannis G, Geibel C, Steglich F, Fulde P and Komatsubara T 2001 *Nature* **410** 340
[7] Thalmeier P 2002 *Eur. Phys. J.* B **27** 29
[8] Zwicknagl G, Yaresko A N and Fulde P 2002 *Phys. Rev.* B **65** R81103
[9] Akazawa T, Hidaka H, Fujiwara T, Kobayashi T C, Yamamoto E, Haga Y, Settai R and Onuki Y 2004 *J. Phys.: Condens. Matter* **16** L29
[10] Rogl P, Bauer J and Debuigne J 1989 *J. Nucl. Mater.* **165** 74
[11] Rogl P and Fischer P 1991 *J. Solid State Chem.* **90** 285
[12] Rogl P and Fischer P 1989 *J. Solid State Chem.* **78** 294
[13] Rogl P, Rupp B, Felner I and Fischer P 1993 *J. Solid State Chem.* **104** 377
[14] Rodriguez-Carvajal J 1993 *Physica* B **192** 55
[15] Sears V F 1992 *Neutron News* **3** 26
[16] Parthé E, Gelato L, Chabot B, Penzo M, Cenzual K and Gladyshevskii R 1994 *TYPIX Standardized Data and Crystal Chemical Characterization of Inorganic Structure Types* (Berlin: Springer)
[17] Slater J C 1937 *Phys. Rev.* **52** 198
[18] Herring C and Kittel C 1951 *Phys. Rev.* **81** 869
[19] Phillips T G and Rosenberg H M 1966 *Rep. Prog. Phys.* **29** 285
[20] Niira K 1960 *Phys. Rev.* **117** 129
[21] Fournier J-M and Troć R 1984 *Handbook on the Physics and Chemistry of the Actinides* ed A J Freeman and G H Lander (Amsterdam: Elsevier Science Publishers B.V.) chapter 2
[22] Paolasini L, Caciuffo R, Roessli B, Lander G H, Myers K and Canfield P 1999 *Phys. Rev.* B **59** 6867
[23] Mook H A 1988 *Spin Waves and Magnetic Excitations I* ed A S Borovik-Romanov and S K Sinha (Amsterdam: Elsevier) p 444
[24] Arrott A and Noakes J E 1967 *Phys. Rev. Lett.* **19** 786
[25] Allen P B and Dynes R C 1975 *Phys. Rev.* B **12** 905
[26] Watanabe S and Miyake K 2002 *Physica* B **312/313** 115
Watanabe S and Miyake K 2002 *J. Phys. Soc. Japan* **71** 2489
[27] Kohn W 1959 *Phys. Rev. Lett.* **2** 393
[28] Fishman R S and Liu S H 1989 *Phys. Rev.* B **40** 11028
[29] Bouvier M, Lethuillier P and Schmitt D 1991 *Phys. Rev.* B **43** 13137
Blanco J A, Gignoux D and Schmitt D 1991 *Phys. Rev.* B **43** 13145
[30] Bauer E, Lackner R, Hilscher G, Michor H, Sieberer M, Eichler A, Gribanov A, Seropegin Y and Rogl P 2005 *J. Phys.: Condens. Matter* **17** 1877
[31] Andersen H H and Smith H 1979 *Phys. Rev.* B **19** 384
[32] Prokeš K, Fujita T, Brück E, de Boer F R and Menovsky A A 1999 *Phys. Rev.* B **60** R730
[33] Tran V H, Czopnik A, Du Plessis P de V, Strydom A M, Troć R and Zaremba V 2000 *J. Phys.: Condens. Matter* **12** 9897
[34] Andreev A V, Diviš M, Javorský P, Prokeš K, Sechovský V, Kunes J and Shiokawa Y 2001 *Phys. Rev.* B **64** 144408
[35] Kaczorowski D, Kruk R, Sanchez J P, Malaman B and Wastin F 1998 *Phys. Rev.* B **58** 9277
[36] Oomi G, Kagayama T and Onuki Y 1998 *J. Alloys Compounds* **271–273** 482
[37] Bauer E D, Freeman E J, Sirvent C and Maple M B 2001 *J. Phys.: Condens. Matter* **13** 5675
[38] Kadowaki K and Woods S B 1986 *Solid State Commun.* **58** 507
[39] Takimoto T and Moriya T 1996 *Solid State Commun.* **99** 457

[40] Miyake K, Matsuura T and Varma C M 1989 *Solid State Commun.* **71** 1149
[41] Custers J, Gegenwar P, Wilhelm H, Neumaier K, Tokiwa Y, Trovarelli O, Geibel C, Steglich F, Pépin C and Coleman P 2003 *Nature* **424** 524
[42] Bianchi A, Movshovich R, Vekhter I, Pagliuso P G and Sarrao J L 2003 *Phys. Rev. Lett.* **91** 257001
[43] Onuki Y, Yun S W, Ukon I, Umehara I, Satoh K, Sakamoto I, Hunt M, Meeson P, Probst P A and Sprinford M 1991 *J. Phys. Soc. Japan* **60** 2127
[44] Troć R, Noël H and Bourlet P 2002 *Phil. Mag.* B **7** 805
[45] Troć R 2003 *Acta Phys. Pol.* B **34** 407
[46] Tran V H, Paschen S, Troć R, Baenitz M and Steglich F 2004 *Phys. Rev.* B **69** 195314
[47] Onuki Y, Ukon I, Yun S W, Umehara I, Satoh K, Fukuhara T, Sato H, Takayanagi S, Shikama M and Ochiai A 1992 *J. Phys. Soc. Japan* **61** 293